50 mL of 0.005 M sodium naphthalenide solution in THF.

Results and Discussion

A variety of strategies were employed to exchange intercalated Cu(II), Ni(II), and Zn(II) with protons from solution and regenerate α-ZrP. Using a 0.5 M HCl solution, the deintercalation reaction was complete within 24 h in all cases and the product solid was found to be poorly crystalline α-ZrP.[12] With less concentrated solutions of HCl, the reaction simply proceeded more slowly, until at 0.01 M the solid remained colored (Cu, Ni) and did not display an X-ray pattern characteristic of α-ZrP after 6 days.

Using acetic acid, no deintercalation reaction was observed, nor was any reaction noted between CH_3COOH and intercalated ions, even after 4 days of reflux in a 1.0 M acid solution.

The most intriguing results were obtained by adding 2.0 mL of acetylacetone to a slurry of 300 mg of CuZrP in 50 mL of water. Within seconds, formation of the deep blue, insoluble $Cu(acac)_2$ complex, characterized by UV-visible and IR spectra, was apparent. At room temperature after 48 h, the deintercalation did not proceed to completion, as evidenced by the blue color of the zirconium phosphate product and persistence of a diffuse diffraction peak at 9.7 Å. However, under reflux for 24 h the blue color disappears and a surprisingly crystalline α-ZrP product is formed. This result was not obtained in the Ni or Zn derivatives, suggesting that the favorable formation of the particularly stable $Cu(acac)_2$ complex drives the deintercalation reaction in that case.

Similarly, when ZnZrP is suspended in a Na(ddtc) solution, crystalline $Zn(ddtc)_2$ is produced, characterized by X-ray powder diffraction, while the diffraction pattern of ZnZrP disappears. No zirconium phosphate phase is apparent in the diffraction pattern due to loss of crystallinity. When CuZrP is suspended in Na(ddtc) solution, a small amount of $Cu(ddtc)_2$ is produced and characterized by UV-visible absorption,[13] presumably by deintercalation at the surfaces of microcrystals, but the powder diffraction pattern of CuZrP remains intact, with no sign of the distinctive strong line pattern of $Cu(ddtc)_2$.[14] These results further indicate the importance of complex formation in the deintercalation reaction.

The reversibility of aqueous transition metal ion intercalation in the presence of a strong acid indicates no strong kinetic barrier to the forward reaction in equation 1, and the position of the equilibrium at varying pH suggests that the equilibrium constant is on the order of 10^1.

$$MZr(PO_4)_2(s) + 2H^+(aq) \leftrightarrow Zr(HPO_4)_2(s) + M^{2+}(aq) \quad (1)$$

However, the introduction of acetylacetone introduces the alternate equilibrium in eq 2, whose equilibrium constant is

$$MZr(PO_4)_2(s) + 2Hacac(aq) \leftrightarrow Zr(HPO_4)_2(s) + M(acac)_2(s) \quad (2)$$

particularly large compared to that of eq 1 for M = Cu. When viewed in the light of the inability of acetic acid to affect the deintercalation, it is clear that the high formation constant of the $Cu(acac)_2$ complex compensates for its lower acidity ($pK_a = 9$) relative to acetic acid ($pK_a = 5$).

To our knowledge, this is the first clear demonstration that the deintercalation reaction can be performed by a relatively weak acid, provided that its conjugate base complexes strongly with the deintercalated guest cation. This evidence also confirms the lack of a significant kinetic barrier to the reaction involving the removal of guest species from the intercalated host and replacement with aqueous H^+.

When ferrocenium-intercalated zirconium phosphate was suspended in a 0.5 M HCl solution for 48 h, no change in appearance or X-ray powder pattern of the solid product was observed. Ferrocenium was observed in the filtrate, presumably due to proton exchange with surface-adsorbed ions, and the absorption at 262 nm ($\epsilon = 7079$)[15] showed that nearly 25% of the total $Fe(Cp)_2^+$ was removed by the acid exchange.

Upon reaction with a 1% Na/Hg amalgam in THF, however, nearly quantitative removal of $Fe(Cp)_2$ was affected. The amount of deintercalated ferrocene was measured at 96-100% by UV absorption at 262 nm and the solid product was noncrystalline. When the reduction was performed with sodium naphthalenide, the degree of deintercalation was monitored by absorption at 440 nm ($\epsilon = 9.1$)[16] and determined to be 100 ± 10%. The solid product was very light brown in color and poorly crystalline, with one weak reflection at 8.64 Å, indicative of a Na^+-intercalated product.[17]

When the surface-exchanged cobaltocenium compound was suspended in THF with a 1% Na/Hg amalgam or sodium naphthalenide, within 2 h the solution turned the distinctive pink color of cobaltocene, indicating reduction of the surface-bound ions. Similar treatment of the fully intercalated product for 24 h also yielded a small amount of desorbed $Co(Cp)_2$, presumably from reduction of surface adsorbed $Co(Cp)_2^+$, but the solid product maintained its appearance and its interlayer spacing of 13.2 Å, indicating no reaction with intercalated cobaltocenium ions. UV absorption at 324 nm ($\epsilon = 17378$)[15] indicated that only 15-25% of the cobaltocenium ions were reduced to cobaltocene.

While the strong and weak acid reactions indicate that metathetical strategies are often sufficient to remove intercalated species, they also indicate that stronger conditions may be necessary. The sodium reactions suggest that controlled reductive (even electrochemical) deintercalations can be useful in removing species which have formed or reacted in the interlayer gallery. Inclusion of reactive species in the inert and protective α-ZrP layers may also prove useful in storage and in limiting reactivity. Solid α-ZrP is truly showing its potential as a "solid solvent" for a variety of chemical purposes.

Acknowledgment. We wish to thank and acknowledge the donors of the Petroleum Research Fund, administered by the American Chemical Society, and the University of Vermont Research Advisory Council for funding support.

Supplementary Material Available: A table of elemental analyses for zirconium phosphate derivatives (1 page). Ordering information is given on any current masthead page.

(12) Note that the Cu, Ni, and Zn derivatives cannot be prepared directly from α-ZrP, due presumably to the kinetic difficulty of expanding the zirconium phosphate galleries from 7.6 Å in α-ZrP.

(13) Choi, S.-N.; Menzel, E. R.; Wasson, J. R. *J. Inorg. Nucl. Chem.* **1977**, *39*, 417.
(14) Fackler, J. P.; Holah, D. G. *Inorg. Nucl. Chem. Lett.* **1966**, *2*, 251.
(15) Gordon, K. R.; Warren, K. D. *Inorg. Chem.* **1978**, *17*, 987.
(16) Sohn, Y. S.; Hendrickson, D. N.; Gray, H. B. *J. Am. Chem. Soc.* **1971**, *93*, 3603.
(17) Clearfield, A.; Duax, W. L.; Medina, A. S.; Smith, G. D.; Thomas, J. R. *J. Phys. Chem.* **1969**, *73*, 3424.

Contribution from the Department of Chemistry, Dalhousie University, Halifax, Nova Scotia, Canada B3H 4J3

Homonuclear ^{31}P *J*-Resolved 2D Spectra of Rhodium(I) Phosphine Complexes in the Solid State

Gang Wu and Roderick E. Wasylishen*

Received June 25, 1991

Introduction

Homonuclear *J*-resolved 2D NMR spectroscopy is one of the basic techniques widely used in solution-state NMR studies;[1] however, the application of this 2D technique has not been extensively used for the study of solid materials.[2-4] In this note we demonstrate the utility of this technique in studying ^{31}P NMR spectra of two square-planar rhodium(I) phosphine complexes of

* To whom all correspondence should be addressed.

0020-1669/92/1331-0145$03.00/0

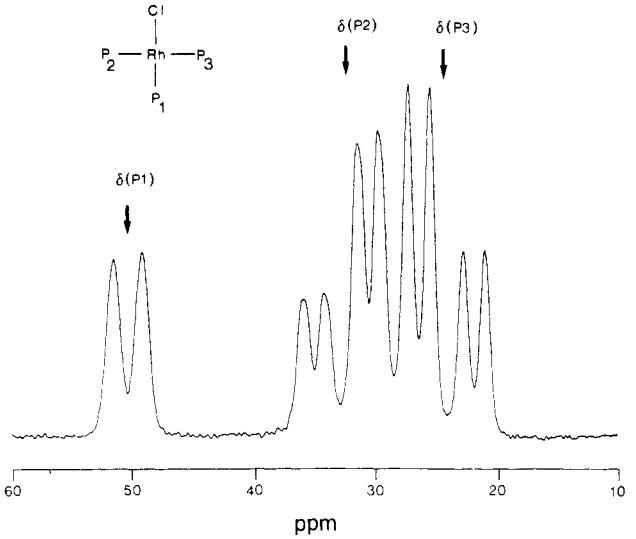

Figure 1. 1D CP/MAS isotropic spectrum of $RhCl(PPh_3)_3$. The sample spinning rate was 4000 Hz, and the recycle time was 10 s. A total of 360 transients were recorded.

catalytic importance, the red polymorph of $RhCl(PPh_3)_3$ (**1**) and *trans*-$Rh(CO)Cl(PPh_3)_2$ (**2**).

Results and Discussion

The 1D CP/MAS ^{31}P NMR spectrum of a solid powder sample of **1** is shown in Figure 1. The three ^{31}P nuclei give rise to the ABM part of an ABMX spin system (X = ^{103}Rh), with the low-field doublet assigned to the phosphorus nucleus, P1, trans to the chlorine atom. The AB pattern due to $^2J(P,P)$ between the two mutually trans ^{31}P nuclei is further split by J coupling to the ^{103}Rh nucleus. Close inspection of the AB multiplet reveals that the low-field half is slightly broader than the high-field half, suggesting the presence of an unresolved cis $^2J(P,P)$ coupling to P1 (i.e., $^2J(P1,P2) > {}^2J(P1,P3)$).

The homonuclear ^{31}P J-resolved 2D spectrum of **1** is shown in Figure 2. For the sake of clarity only the first low-frequency spinning sidebands are shown, since there are additional strong J-coupling signals in the isotropic region.[5] We shall discuss such strong J-coupling signals in our second example. In the ^{31}P homonuclear J-resolved 2D spectrum of $RhCl(PPh_3)_3$, the heteronuclear J couplings due to $^1J(Rh,P)$ remain along the f_2 dimension while the homonuclear J couplings between ^{31}P nuclei appear along the f_1 dimension. All the isotropic data reported by a previous 1D CP/MAS study[6] were confirmed by our 1D and 2D spectra. Analysis of our spectra yields δ(P1) = 50.5 ppm, δ(P2) = 32.3 ppm, δ(P3) = 24.8 ppm, $^1J(Rh,P1) = -191$ Hz, $^1J(Rh,P2) = -139$ Hz, $^1J(Rh,P3) = -146$ Hz, and $^2J(P2,P3) = +366$ Hz. The signs of the J couplings cannot be determined from our 1D and 2D spectra; they are taken to be the same as those obtained

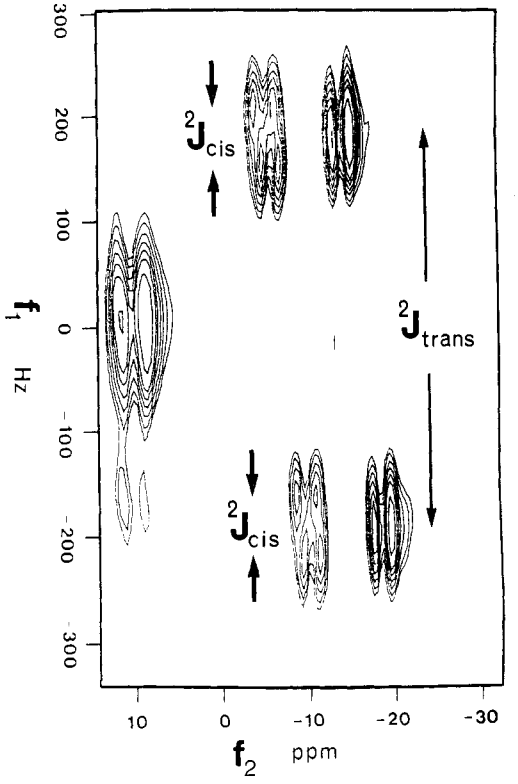

Figure 2. J-resolved 2D spectrum of $RhCl(PPh_3)_3$. Since the signals shown are the first low-frequency spinning sideband, they are shifted from their isotropic positions by 40.1 ppm. The sample spinning rate was 3250 ± 5 Hz, and the t_1 increment was 0.62 ms. A total of 32 t_1 increments were acquired and zero-filled to 64 words in the f_1 dimension prior to Fourier transformation. The data matrix was 64 × 2K. The recycle time was 10 s. Sine bell functions were applied to both dimensions prior to the 2D FT. The spectrum was not tilted, and therefore no J symmetrization was applied. The total time to acquire the 2D spectrum was 5.6 h.

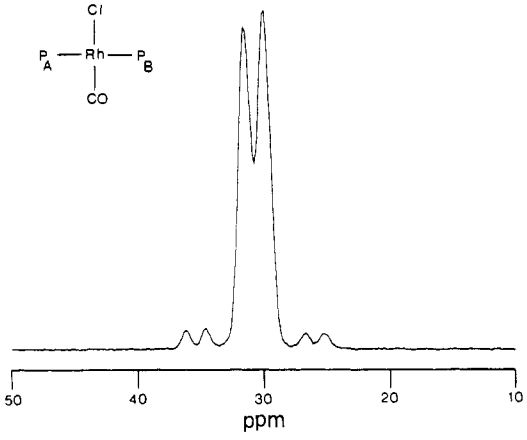

Figure 3. Isotropic part of CP/MAS 1D spectrum of *trans*-$Rh(CO)Cl(PPh_3)_2$. The sample spinning rate was 4000 Hz, and the recycle time was 10 s. A total of 100 transients were recorded.

for related compounds from previous NMR studies.[7,8]

The most striking observation in the J-resolved 2D spectrum of **1** is that one of the two-bond ^{31}P–^{31}P cis couplings, $^2J(P1,P2)$, is well-resolved. This cis coupling constant is 58 ± 5 Hz, which is substantially larger than that observed in the solution state, 38 Hz.[9] The other cis coupling, $^2J(P1,P3) \leq 30$ Hz, is to small to be resolved in the solid state. In contrast to the solution case, where

(1) (a) Ernst, R. R.; Bodenhausen, G.; Wokaun, A. *Principles of Nuclear Magnetic Resonance in One and Two Dimensions*; Oxford University Press: Oxford, U.K., 1987. (b) Derome, A. D. *Modern NMR Techniques for Chemistry Research*; Pergamon Press: Oxford, U.K., 1987. (c) Sanders, J. K. M.; Hunter, B. K. *Modern NMR Spectroscopy: A Guide for Chemists*; Oxford University Press: Oxford, U.K., 1987. (d) Bax, A.; Lerner, L. *Science* **1986**, *232*, 960.
(2) Allman, T. *J. Magn. Reson.* **1989**, *83*, 637.
(3) Kubo, A.; McDowell, C. A. *J. Chem. Phys.* **1990**, *92*, 7156.
(4) Challoner, R.; Nakai, T.; McDowell, C. A. *J. Chem. Phys.* **1991**, *94*, 7038.
(5) In the 1D ^{31}P CP/MAS spectrum of compound **1**, it was noted that the multiplets in the first- and second-order spinning sidebands showed much less AB character than the isotropic multiplet shown in Figure 1; thus, the intensity of the additional peaks in the 2D spectra due to strong coupling effects was significantly minimized in the first-order spinning sidebands. Although a complete description of the relative intensities of J-coupled multiplets in different-order MAS sidebands is beyond the scope of the present paper, it is clear that the mixing term, $D = [(\delta_A - \delta_B)^2 + J_{AB}^2]^{1/2}$, is orientation dependent and therefore time dependent in rotating solids.
(6) Diesveld, J. W.; Menger, E. M.; Edzes, H. T.; Veeman, W. S. *J. Am. Chem. Soc.* **1980**, *102*, 7935.
(7) Hyde, E. M.; Kennedy, J. D.; Shaw, B. L.; McFarlane, W. *J. Chem. Soc., Dalton Trans.* **1977**, 1571.
(8) Pregosin, P. S.; Kunz, R. W. In *NMR Basic Principles and Progress*; Diehl, P., Fluck, E., Kosfeld, R., Eds.; Springer-Verlag: Berlin, 1979.

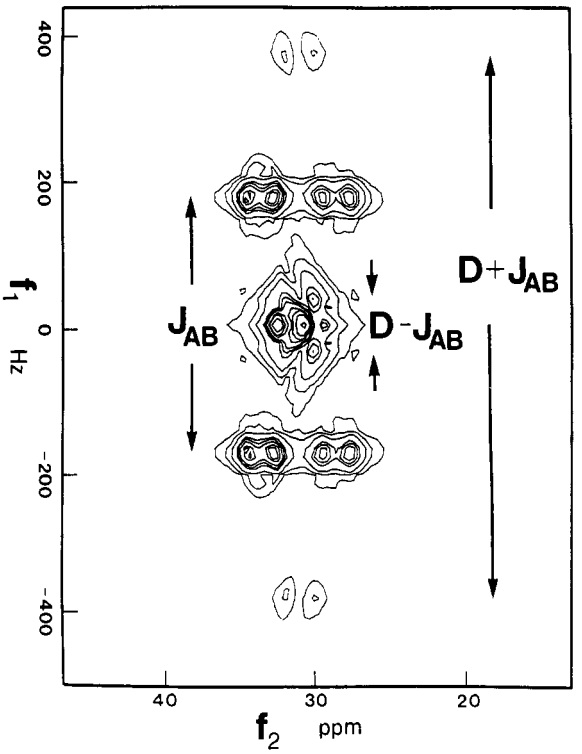

Figure 4. Isotropic part of the 2D *J*-resolved spectrum of *trans*-Rh(CO)Cl(PPh_3)$_2$. The spinning rate was 3125 ± 5 Hz, and the t_1 increment was 0.64 ms. A total of 64 increments in f_1 were recorded and zero-filled to 128 words prior to Fourier transformation. The whole data matrix was 128 × 2K. The recycle time was 10 s. Sine bell functions were applied to both dimensions prior to 2D FT. The spectrum was tilted 45° and symmetrized. The total time to acquire the 2D spectrum was 5.6 h.

the two mutually trans phosphorus nuclei are equivalent and only one cis ^{31}P–^{31}P coupling constant can be observed,[9] two quite different cis couplings are found in solid RhCl(PPh_3)$_3$, indicating some subtle difference in the geometric structure at the two sites. The conclusion that the two mutually trans phosphorus nuclei are nonequivalent in the solid state is supported by X-ray diffraction results.[10]

The 1D CP/MAS ^{31}P NMR spectrum of a solid powder sample of *trans*-Rh(CO)Cl(PPh_3)$_2$ (**2**) is given in Figure 3. The ^{31}P NMR spectrum forms a tightly coupled AB part of an ABX spin system (X = ^{103}Rh). The splittings in the weak outer doublets are equal, 125 Hz, indicating $^1J(Rh,P_A) = {}^1J(Rh,P_B)$. Since the two ^{31}P nuclei are tightly *J*-coupled, the two inner lines of the AB pattern are not resolved. Therefore, both the $^2J(P,P)$ coupling constant and the isotropic ^{31}P chemical shifts cannot be directly obtained from the 1D spectrum. However, from the homonuclear ^{31}P *J*-resolved 2D spectrum of **2**, shown in Figure 4, one can directly determine the value of $^2J(P,P)$ and thus the two isotropic chemical shifts. Analysis of the 1D and 2D spectra yields the following parameters: $\delta(P_A)$ = 29.5 ppm, $\delta(P_B)$ = 31.9 ppm, $^1J(Rh,P_A) = {}^1J(Rh,P_B) = -125$ Hz, and $^2J(P_A,P_B) = +360$ Hz. Again, the signs of the *J* couplings are based on those determined for related compounds.[7,8] Since the two triphenylphosphine ligands in **2** are equivalent in solution, $^2J(P,P)$ cannot be measured.[9] In the solid state, however, the two phosphorus sites are nonequivalent[11] and permit measurement of $^2J(P,P)$. It is interesting to note the presence of additional signals which arise from strong *J* coupling between the two ^{31}P nuclei. The positions of the strong coupling signals found in our solid-state 2D spectra are in agreement with predictions for an AB spin system in solution-state NMR studies.[12-14] In the f_1 dimension the separation between the outer lines due to the strong coupling effect is equal to $D + J_{AB}$, where $D = [(\delta_A - \delta_B)^2 + J_{AB}^2]^{1/2}$, while the two inner lines are separated by $D - J_{AB}$. Since a strong peak appears at f_1 = 0, the two inner lines are partially obscured.

One of the advantages of using *J*-resolved 2D experiments in solution-state NMR studies is to improve the resolution along the f_1 dimension, by refocusing the magnetization dephased due to an inhomogeneous magnetic field. In the solid state, however, there are several intrinsic sources of residual line broadening under the condition of magic angle spinning.[15] In contrast to solution-state NMR spectroscopy, the line broadening due to an inhomogeneous field is usually not a significant factor for the solid samples (the magnetic field inhomogeneity contributes less than 4 Hz to the ^{31}P NMR line widths on our spectrometer, compared with the observed line width of about 90 Hz in the 1D CP/MAS ^{31}P NMR spectra of our rhodium(I) phosphine complexes). In fact, the homonuclear dipolar interactions between the ^{31}P nuclei, the heteronuclear dipolar interactions between the ^{31}P and ^{103}Rh nuclei, and the anisotropic ^{31}P chemical shifts play more important roles in broadening the lines of an MAS spectrum. The spin-echo technique used in the *J*-resolved 2D experiments, however, takes advantage of the fact that at the top of each echo both the heteronuclear dipolar interaction and the anisotropic chemical shift are refocused. Thus superior resolution is achieved in the f_1 dimension. This resolution in f_1 is merely determined by the magnitude of the ^{31}P homonuclear dipolar interactions (here we ignore those factors that an experimentalist can control, e.g. rotor stability, magic angle setting, proton decoupling power, etc.). This mechanism of improving the resolution in the f_1 dimension of a *J*-resolved 2D spectrum for solid samples seems not to have been fully appreciated previously. It is a general observation that the line widths are nearly linear with applied magnetic field strength,[16] and therefore a high field is not desirable for measurement of the fine structure due to *J* couplings. However, as we have discussed, the line widths in the f_1 dimension of the *J*-resolved 2D spectrum are, in principle, independent of field. Although a similar improvement in resolution can also be accomplished by the 1D rotation-synchronized CPMG spin-echo experiment on solid samples,[17] the advantage of the 2D *J*-resolved experiment is obvious.

Another important consideration in applying the 2D *J*-resolved experiment to solid samples rotating at the magic angle is that the sampling in the t_1 dimension must satisfy the condition $t_1 = 2nT_R$, where n is an integer and T_R is the rotor period, so that all spinning sidebands in the f_1 dimension become coincident, enhancing the 2D signals. Although the spinning sidebands in the f_1 dimension may be of importance in some cases,[18] they are not desirable in the present study.

Experimental Section

The pulse sequence used in this study was CP(ϕ_1)–t_1/2–π-($^{31}P,\phi_2$)–t_1/2–ACQ(ϕ_3,t_2). High-power proton decoupling was applied in both the t_1 evolution and the t_2 detection periods. A simple eight-step phase cycling scheme of $\phi_1 = \phi_2 = +Y, +Y, +X, +X, -Y, -Y, -X, -X$ and $\phi_3 = +Y, -Y, +X, -X, -Y, +Y, -X, +X$ was used, with the initial ^1H 90° pulse in the CP segment altering between $+Y$ and $-Y$. The t_1 increment was synchronized with the sample rotation period. The spectral width and the number of points along the f_1 dimension were varied in order to give acceptable digital resolution and total data accumulation time. The 180° pulse width for ^{31}P was measured as 7.5 μs. A typical contact time for the cross-polarization was 5 ms. All spectra were recorded on a Bruker MSL-200 NMR spectrometer operating at 81.033 MHz for ^{31}P and were referenced with respect to 85% H_3PO_4(aq).

(9) Brown, T. H.; Green, P. J. *J. Am. Chem. Soc.* **1970**, *92*, 2359.
(10) Bennett, M. J.; Donaldson, P. B. *Inorg. Chem.* **1977**, *16*, 655.
(11) Del Pra, A.; Zanotti, G.; Segala, P. *Cryst. Struct. Commun.* **1979**, *8*, 959.
(12) Kumar, A. *J. Magn. Reson.* **1978**, *30*, 227.
(13) Bodenhausen, G.; Freeman, R.; Morris, G. A.; Turner, D. L. *J. Magn. Reson.* **1978**, *31*, 75.
(14) Kay, L. E.; McClung, R. E. D. *J. Magn. Reson.* **1988**, *77*, 258.
(15) Brunner, E.; Freude, D.; Gerstein, B. C.; Pfeifer, H. *J. Magn. Reson.* **1990**, *90*, 90.
(16) Alla, M.; Lippmaa, E. *Chem. Phys. Lett.* **1982**, *87*, 30.
(17) Harris, R. K.; Sebald, A. *Magn. Reson. Chem.* **1989**, *27*, 81.
(18) Kolbert, A. C.; Raleigh, D. P.; Levitt, M. H.; Griffin, R. G. *J. Chem. Phys.* **1989**, *90*, 679.

All 2D spectra were obtained in the absolute-value mode.

Summary

In summary, the high sensitivity and the high resolution of ^{31}P NMR signals usually obtained by the combination of cross-polarization, magic angle, and high-power proton-decoupling techniques provide a sound base for feasible 2D *J*-resolved experiments. Since the pulse sequence and spectral interpretation in the solid state are directly analogous to those in solution, homonuclear ^{31}P *J*-resolved 2D NMR spectroscopy has the potential to become a routine technique for chemists interested in solid materials such as metal phosphine complexes. Also, the experiment could be easily extended to give a heteronuclear ^{31}P–^{103}Rh *J*-resolved 2D spectrum if a triply tuned probe were available. Further work is in progress in our laboratory.

Acknowledgment. We are grateful to the NSERC of Canada for financial support.

Registry No. $RhCl(PPh_3)_3$, 14694-95-2; *trans*-$Rh(CO)Cl(PPh_3)_2$, 15318-33-9.

Contribution from the Department of Chemistry, University of Pennsylvania, Philadelphia, Pennsylvania 19104-6323

Reactions of H_2 (D_2) with a Rhodium(II) Metalloradical: Kinetic Evidence for a Four-Centered Transition State

Bradford B. Wayland,* Sujuan Ba, and Alan E. Sherry

Received July 13, 1991

Metal-catalyzed hydrogenation of substrates involves addition of hydrogen to the metal center as an obligatory step.[1] The importance of this class of reactions has stimulated efforts to understand the scope of mechanistic pathways operative in reactions of H_2 with metal complexes. Formation of dihydrides by addition to a single metal center ($M + H_2 \rightarrow M(H)_2$) and monohydrides by reaction with two metal sites ($2M + H_2 \rightarrow 2MH$) are both frequently observed.[2] Concerted addition of H_2 to form dihydrides through a three-centered triangular transition state has been thoroughly documented by kinetic studies,[3-5] observation of η^2-dihydrogen complexes,[6] and theoretical considerations.[7] Formation of monohydrides by addition of H_2 to two metal centers is less fully investigated, but both multistep heterolytic[8] and concerted homolytic[9-12] cleavage of dihydrogen have been recognized. This article describes the reaction of H_2 (D_2) with (tetramesitylporphyrinato)rhodium(II),[13] (TMP)Rh• (**1**), to form (TMP)Rh–H through a four-centered transition state.

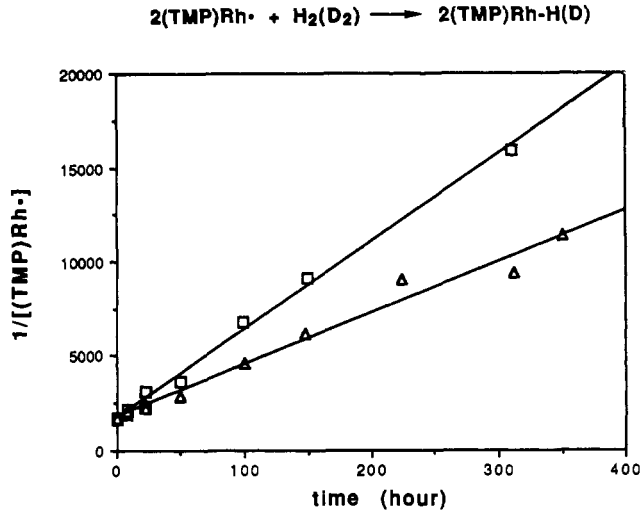

Figure 1. Representative second-order kinetic plots for the reaction of (TMP)Rh• with H_2 (□) and D_2 (△) in C_6D_6 at 296 K ($[(TMP)RH^•]_i = (5.9 \pm 0.1) \times 10^{-4}$ M; $P_{H_2} = P_{D_2} = 0.838 \pm 0.002$ atm; $[H_2] = 2.40 \times 10^{-3}$ M) (k_{H_2}(296 K) = 2.7 L^2 mol^{-2} s^{-1}; k_{D_2}(296 K) = 1.6 L^2 mol^{-2} s^{-1}; k_{H_2}/k_{D_2}(296 K) = 1.7).

Results

Benzene solutions of (TMP)Rh• (**1**) ($\sim 5 \times 10^{-4}$ M) react with H_2 (P_{H_2} = 0.2–1.0 atm) to form the hydride complex (TMP)Rh–H (**2**) (eq 1), which is identified in solution by ^1H NMR spectroscopy

$$2(TMP)Rh^• + H_2 \rightleftharpoons 2(TMP)Rh\text{–}H \qquad (1)$$

of the characteristic hydride resonance (δ_{Rh-H} = −39.99 ppm; $J_{^{103}Rh-H}$ = 44 Hz) and in the solid state by IR spectroscopy of the Rh–H stretching vibration (ν_{Rh-H} = 2095 cm^{-1}). Reaction 1 proceeds effectively to completion as observed by ^1H NMR spectroscopy for the range of conditions investigated ($[(TMP)Rh^•] = (3–5) \times 10^{-4}$ M; P_{H_2} = 0.2–1.0 atm; T = 296–373 K) which is expected for a reaction of H_2 that forms a hydride complex with a Rh–H bond energy of ~60 kcal mol^{-1}.[13] Reaction 1 is well suited for kinetic studies because it is free from any competitive processes such as solvent reactions, M–M bond formation, and hydrogenation of the ligand, which have complicated previous studies of H_2 reactions with metalloradicals.[10-12] The rate for reaction 1 is observed to have a second-order dependence on the molar concentration of (TMP)Rh• at conditions where the process is pseudo zero order in hydrogen (Figure 1). Second-order rate plots are linear throughout the entire reaction time, as required for a process that proceeds effectively to completion (Figure 1). Variation of the H_2 concentration (P_{H_2}(296 K) = 0.2–0.9 atm.) demonstrates a first-order rate dependence on the molar concentration of H_2 and an overall third-order rate law for reaction 1 ($rate_1 = k_1[(TMP)Rh^•]^2[H_2]$). Temperature dependence of the third-order rate constant (k_1) was used in deriving estimates for the transition-state and Arrhenius activation parameters

(1) (a) James, B. R. *Comprehensive Organometallic Chemistry*; Wilkinson, G., Stone, F. G. A., Abel, E. W., Eds.; Pergamon: New York, 1982; Vol. 8, p 285. (b) Jardine, F. H. *Prog. Inorg. Chem.* **1981**, *28*, 63. (c) Faller, J. W. *Homogeneous Catalysis with Metal Phosphine Complexes*; Pignolet, L. H., Ed.; Plenum: New York, 1983; Chapter 2.
(2) Collman, J. P.; Hegedus, L. S.; Norton, J. R.; Finke, R. G. *Principles and Applications of Organotransition Metal Chemistry*; University Science Books: Mill Valley, CA, 1987; p 286.
(3) Chock, P. B.; Halpern, J. *J. Am. Chem. Soc.* **1966**, *88*, 3511.
(4) Zhou, P.; Vitale, A. A.; San Filippo, J., Jr.; Saunders, W. H., Jr. *J. Am. Chem. Soc.* **1985**, *107*, 8049.
(5) (a) Johnson, C. E.; Eisenberg, R. *J. Am. Chem. Soc.* **1985**, *107*, 6531. (b) Kunin, A. J.; Farid, R.; Johnson, C. E.; Eisenberg, R. *J. Am. Chem. Soc.* **1985**, *107*, 5315. (c) Wink, D.; Ford, P. C. *J. Am. Chem. Soc.* **1985**, *107*, 1794.
(6) (a) Kubas, G. J.; Ryan, R. R.; Swanson, B. I.; Vergamini, P. J.; Wasserman, H. J. *J. Am. Chem. Soc.* **1984**, *106*, 451. (b) Morris, R. H.; Sawyer, J. F.; Shiralain, M.; Zubkowski, J. D. *J. Am. Chem. Soc.* **1985**, *107*, 5581. (c) Crabtree, R. H.; Lavin, M. *J. Chem. Soc., Chem. Commun.* **1985**, 794. (d) Sweany, R. L. *Organometallics* **1986**, *5*, 387. (e) Collman, J. P.; Wagenknecht, P. S.; Hembre, R. T.; Lewis, N. S. *J. Am. Chem. Soc.* **1990**, *112*, 1294. (f) Collman, J. P.; Hutchison, J. E.; Wagenknecht, P. S.; Lewis, N. S.; Lopez, M. A.; Guilard, R. *J. Am. Chem. Soc.* **1990**, *112*, 8206.
(7) (a) Sailliard, J.-Y.; Hoffman, R. *J. Am. Chem. Soc.* **1984**, *106*, 2006. (b) Nakatsuji, H.; Hada, M. *J. Am. Chem. Soc.* **1985**, *107*, 8264. (c) Siegbahn, P. E. M.; Blomberg, M. R. A.; Bauslicher, C. W., Jr. *J. Chem. Phys.* **1984**, *81*, 1373. (d) Low, J. J.; Goddard, W. A., III. *J. Am. Chem. Soc.* **1984**, *106*, 8321. (e) Obara, S.; Kitaura, K.; Morkuma, K. *J. Am. Chem. Soc.* **1984**, *106*, 7482.
(8) (a) Brothers, P. J. *Prog. Inorg. Chem.* **1980**, *28*, 1. (b) Fachinetti, G.; Del Cima, F.; Braca, G. F.; Funaioli, T. *J. Organomet. Chem.* **1984**, *275*, C25. (c) Sisak, A.; Ungvary, F.; Marko, L. *Organometallics* **1983**, *2*, 1244.
(9) (a) Halpern, J.; Pribanic, M. *Inorg. Chem.* **1970**, *9*, 2616. (b) Halpern, J. *Inorg. Chim. Acta* **1983**, *77*, L105.
(10) Halpern, J. *Inorg. Chim. Acta* **1982**, *62*, 31.
(11) Simandi, L. I.; Budo-Zahony, E.; Szvernyi, Z.; Memeth, S. *J. Chem. Soc., Dalton Trans.* **1980**, 276.
(12) Chao, T.-H.; Espenson, J. H. *J. Am. Chem. Soc.* **1978**, *100*, 129.
(13) (a) Sherry, A. E.; Wayland, B. B. *J. Am. Chem. Soc.* **1990**, *112*, 1259. (b) Wayland, B. B.; Ba, S.; Sherry, A. E. *J. Am. Chem. Soc.* **1991**, *113*, 5305.

0020-1669/92/1331-0148$03.00/0